

Article

An Improved Artificial Ecosystem-Based Optimization Algorithm for Optimal Design of a Hybrid Photovoltaic/Fuel Cell Energy System to Supply A Residential Complex Demand: A Case Study for Kuala Lumpur

Jing Yang ¹, Yen-Lin Chen ^{2,*}, Por Lip Yee ^{1,*}, Chin Soon Ku ^{3,*} and Manoochehr Babanezhad ⁴

¹ Department of Computer System and Technology, Faculty of Computer Science and Information Technology, Universiti Malaya, Kuala Lumpur 50603, Malaysia

² Department of Computer Science and Information Engineering, National Taipei University of Technology, Taipei 106344, Taiwan

³ Department of Computer Science, Universiti Tunku Abdul Rahman, Kampar 31900, Malaysia

⁴ Department of Statistics, Faculty of Sciences, Golestan University, Gorgan 49138-15759, Iran

* Correspondence: ylchen@mail.ntut.edu.tw (Y.-L.C.); porlip@um.edu.my (P.L.Y.); kucs@utar.edu.my (C.S.K.)

Abstract: In this paper, the optimal design of a hybrid energy system (HES), consisting of photovoltaic technology integrated with fuel cells (HPV/FC) and relying on hydrogen storage, is performed to meet the annual demand of a residential complex to find the minimum total net present cost (TNPC), while observing the reliability constraint as the energy-not-supplied probability (ENSP) and considering real meteorological data of the Kuala Lumpur city in Malaysia. The decision variables include the size of system components, which are optimally determined by an improved artificial ecosystem-based optimization algorithm (IAEO). The conventional AEO is improved using the dynamic lens-imaging learning strategy (DLILS) to prevent premature convergence. The results demonstrated that the decrease (increase) of the reliability constraint leads to an increase (decrease) in the TNPC, as well as the cost of electricity (COE). For a maximum reliability constraint of 5%, the results show that the TNPC and COE obtained USD 2.247 million and USD 0.4046 million, respectively. The superior performance of the IAEO has been confirmed with the AEO, particle swarm optimization (PSO), and manta ray foraging optimization (MRFO), with the lowest TNPC and higher reliability. In addition, the effectiveness of the hydrogen tank efficiency and load changes is confirmed in the hybrid system design.

Keywords: HPV/FC energy system; optimal design; energy-not-supplied probability; dynamic lens-imaging learning strategy; improved artificial ecosystem-based optimization



Citation: Yang, J.; Chen, Y.-L.; Yee, P.L.; Ku, C.S.; Babanezhad, M. An Improved Artificial Ecosystem-Based Optimization Algorithm for Optimal Design of a Hybrid Photovoltaic/Fuel Cell Energy System to Supply A Residential Complex Demand: A Case Study for Kuala Lumpur. *Energies* **2023**, *16*, 2867. <https://doi.org/10.3390/en16062867>

Academic Editor: Alberto Reatti

Received: 14 February 2023

Revised: 17 March 2023

Accepted: 18 March 2023

Published: 20 March 2023



Copyright: © 2023 by the authors. Licensee MDPI, Basel, Switzerland. This article is an open access article distributed under the terms and conditions of the Creative Commons Attribution (CC BY) license (<https://creativecommons.org/licenses/by/4.0/>).

1. Introduction

The reduction of fossil resources in the world has caused the need for alternative energy sources to become very important [1]. Photovoltaic (PV) energy is a promising source of energy due to its abundance and availability. Nevertheless, the dependence of photovoltaic energy sources on weather conditions and their unpredictability, as well as the lack of proportion between energy demand and supply, are three of the important challenges of using this type of source [2,3]. The storage devices can compensate for the power fluctuations of photovoltaic sources and lead to the creation of programmable power [4,5]. On the other hand, another important storage source that is welcome in a hybrid system is the hydrogen-based fuel cell [6–8]. For effective and economical use of a hybrid renewable energy system, the use of an optimization method is required to solve the design problem, i.e., determine the optimal size of the equipment [9–11]. It should also be noted that the climate and weather significantly impact the design costs and reliability level of the load.

The optimal design of the hybrid system has been widely discussed in previous literature. Ref. [12] presents the optimal structure of a hybrid photovoltaic/wind/battery energy system to minimise electricity costs by satisfying the reliability constraint with the help of the Firefly algorithm. In [13], a hybrid photovoltaic, wind, and battery energy system is optimally designed via combined genetic–particle swarm optimization to minimise the power generation cost and satisfy the reliability constraint. In [14], the design of the energy system, including photovoltaic, diesel, and battery banks, is developed in Algeria to meet an annual demand and minimise the energy cost and load reliability. Ref. [15] optimally designs a photovoltaic, wind, and hydrogen energy system in Iran to supply a residential load by minimising the cost of the useful life of the project using the grey wolf-sine cosine optimization algorithm. In another study, photovoltaic, wind, battery, and diesel energy systems for different regions of Bangladesh were optimally designed using the Homer software, considering energy cost minimization [16]. In [17], a similar approach is adopted for a hybrid photovoltaic/biomass energy system with hydrogen storage to meet a grid-disconnected load in terms of minimising the cost of electricity in Iran via a whale optimization algorithm. In [18], the optimal structure of a photovoltaic, battery, or diesel energy system to minimise the energy production costs and consider the reliability constraint is determined based on the particle swarm optimization in Saudi Arabia. In [19], a PV, wind, battery, and diesel energy system is optimally established to minimise the useful life cost of the project and is investigated to supply off-grid loads using the nomadic people optimization algorithm in Iraq. In [20], a photovoltaic/fuel cell design to minimise the energy cost is evaluated for China using the fractional-order neural network algorithm. In [21], a photovoltaic, wind, and battery system equipped with a diesel backup source is studied to minimise the energy cost and satisfy reliability by adopting an improved grey wolf optimizer in Egypt. In [22], the design of a photovoltaic, wind, and battery energy system to minimise the total net present cost was implemented in Iran using the grasshopper optimization algorithm. In [23], the design of a photovoltaic, fuel cell, or diesel energy system was performed to find the minimum total net present cost and consider the probability of not supplying the load using the crow search algorithm for Iran. In [24], the implementation of a wind/fuel cell energy system with the aim of cost minimization was implemented in China using the elephant herding optimization algorithm. In [25], the design of a photovoltaic/fuel cell energy system is implemented to find the minimum energy cost using a hybrid particle swarm–artificial bee algorithm in India. In [26], a photovoltaic, fuel cell, and diesel generator system is proposed to minimise the TNPC using the search algorithm used in Iran. In [27], the design of a photovoltaic, wind, or battery energy system is discussed to find the minimum levelized energy cost using a genetic algorithm in Morocco. In [28], the design of a photovoltaic, wind, and fuel cell energy system to minimise the total annual cost and consider reliability is implemented in Pakistan using the Jaya algorithm. In [29], a photovoltaic/diesel design with a fuel cell is presented with energy cost minimization via the Mayfly optimization algorithm in Egypt.

A literature review has shown that in many studies, the battery, which is short-term storage, has been used as a storage system. Therefore, the use of long-term fuel cell storage based on hydrogen, which has higher reliability than battery storage, is proposed in the design of the hybrid system in this study. The studies presented in the literature have shown that the use of meta-heuristic algorithms in solving energy system design problems is very important when calculating the optimal scale and capacity of the components.

The present research designs an HPV/FC energy system to supply the annual electrical demand of a residential complex and is performed to minimise the total net present cost based on the meteorological data of the city of Kuala Lumpur in Malaysia using an improved artificial ecosystem-based optimization algorithm (IAEO) to determine the optimal size of the system components. The proposed algorithm is an improved version of the conventional AEO algorithm [30] and is strengthened by using a dynamic lens-imaging learning strategy [31] against premature convergence. The most acceptable arrangement of the hybrid system for different values of the reliability constraint in the city of Kuala

Lumpur has been determined, and the values of the cost of supplying each kWh of energy for the residential complex, along with the reliability indices, have also been calculated.

The rest of the structure of the paper is presented as follows: In Section 2, the HES components are modelled. The design problem includes cost and reliability models, which are presented in Section 3. In Section 4, the suggested method and its procedure are described. In Section 5, the steps of IEOA implementation are presented. Section 6 provides the simulation results, and the paper findings are summarised in Section 7.

2. Hybrid Energy System Modelling

In this study, the design of a hybrid photovoltaic/fuel cell (HPV/FC) energy system is presented to supply the annual demand of a residential complex based on the meteorological data of the city of Kuala Lumpur in Malaysia. The schematic of the HPV/FC system is depicted in Figure 1.

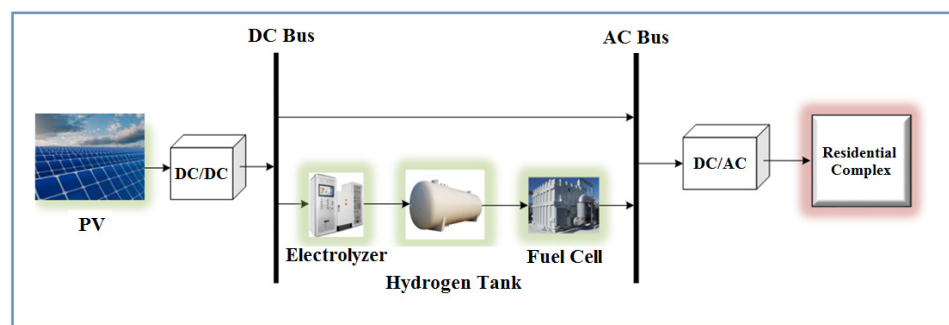


Figure 1. Schematic of HPV/FC energy system.

2.1. HPV/FC Energy System Modeling

2.1.1. PV Model

The production power of a PV panel depends on factors such as the solar radiation irradiated on the panel surface and the ambient temperature. Equation (1) expresses the power generation by a PV [14]:

$$P_{PV} = P_{PV,nom} \times \frac{I_r}{I_{r_{ref}}} \times [1 + N_{TC}(T_{em_c} - T_{em_{Stc}})] \tag{1}$$

$$T_c = T_A + \left[\frac{(NOCT - 20)}{800} \times I_r \right] \tag{2}$$

where $P_{PV, rated}$ indicates the nominal power of the PV unit; I_r and $I_{r_{ref}}$ refer to instantaneous radiation and radiation in the standard condition, respectively; N_{TC} is the PV temperature coefficient (-3.7×10^{-3} (1/°C)); T_{em_c} , $T_{em_{Stc}}$ and T_A refer to the cell, standard condition, and ambient temperature, respectively. $NOCT$ is the temperature of the rated operating cell (°C).

Therefore, taking into account the number of panels (N_{PV}) and the converter efficiency ($\eta_{DC/DC}$), the PV output power in the HES at time t ($P_{PV}^T(t)$) is obtained as follows:

$$P_{PV}^T(t) = \eta_{DC/DC} \times \sum_{n_{PV}=1}^{N_{PV}} P_{PV}(t) \tag{3}$$

2.1.2. Electrolyser

The electrolyser produces hydrogen by delivering power based on the water electrolysis process, whose equation is presented below.

$$P_{El-HST}(t) = P_{PV-El}^T(t) \times \eta_{El} \tag{4}$$

where $P_{El-HST}(t)$ is the electrolyzer output power at time t , $P_{PV-El}^T(t)$ is the injected power of PV to the electrolyser, and η_{El} is the electrolyser efficiency.

2.1.3. Hydrogen Storage Tank

The energy of the tank at time t is obtained as follows [15]:

$$E_{HST}(t) = E_{HST}(t-1) + P_{El-HST}(t) \cdot \Delta t - P_{HST-FC}(t) \cdot \Delta t \times \eta_{HST} \quad (5)$$

$$M_{HST}(t) = E_{HST}(t) / HHV_{H2} \quad (6)$$

where $E_{HST}(t-1)$ indicates the energy of the HST at time $(t-1)$, $P_{El-HST}(t)$ clears the electrolyser output power at time t , $P_{HST-FC}(t)$ is the equivalent power to the hydrogen transferred to the fuel cell, Δt are time steps (1 h intervals), η_{HST} is the efficiency of the HST , $E_{HST}(t) / HHV_{H2}$ denotes the stored hydrogen mass in the HST [15].

2.1.4. Fuel Cell

The fuel cell is used to compensate for the lack of power required by the load in the hybrid system [15].

$$P_{FC-Inv}(t) = P_{HST-FC}(t) \times \eta_{FC} \quad (7)$$

where η_{FC} refers to fuel cell efficiency.

2.1.5. Inverter

The transferred power to the residential complex by the inverter is defined by [15].

$$P_{Inv-CB}(t) = (P_{FC-Inv}(t) + P_{PV-Inv}^T(t)) \times \eta_{Inv} \quad (8)$$

where $P_{Inv-CB}(t)$ is the power transferred by the inverter to the residential complex at time t , and $P_{PV-Inv}^T(t)$ indicates the injected PV power to the inverter.

3. Designing Problem

3.1. Cost Model

The total present value cost includes the initial investment costs (C^{CAP}), maintenance and operation costs (C^{MAIN}), and replacement costs (C^{REP}) of the equipment, which are defined as follows [15,32].

$$\text{Min. } TNPC = NPC^{PV} + NPC^{El} + NPC^{HST} + NPC^{FC} + NPC^{Inv} \quad (9)$$

For each PV source equipment, electrolyser, HST , FC , and NPC inverter, it is defined as follows:

$$NPC^{com} = N^{com} \times (CC^{com} + RC_{npv}^{com} + OM_{npv}^{com}) \quad (10)$$

where com is the type of equipment, N^{com} is the amount of com equipment, CC^{com} is the investment cost of the com equipment, RC^{com} is the replacement cost of the com equipment, and OM^{com} is the net present cost of the operation and maintenance costs of the com equipment.

For com equipment, if OM_{com}^y is the cost of operation and maintenance, the OM_{npv}^{com} value is defined as follows [15]:

$$OM_{npv}^{com} = OM_{com}^y \times \sum_{n=1}^N \frac{1}{(1+r)^n} \quad (11)$$

where r represents the interest rate.

Therefore, the replacement cost of the equipment only for the fuel cell and inverter is presented as follows [15,32]:

$$RC_{npv}^{FC} = RC_{FC} \times \sum_{n=5,10,15,20} \frac{1}{(1+r)^n} \quad (12)$$

$$RC_{npv}^{Inv} = RC_{Inv} \times \sum_{n=10,20} \frac{1}{(1+r)^n} \quad (13)$$

where RC_{FC} and RC_{Inv} are the cost of replacing the fuel cell and inverter, respectively.

3.2. Reliability Model

In this paper, reliability is defined as the energy-not-supplied probability (ENSP). Along with this condition, two loss of energy expectation (LOEE) and loss of load expectation (LOLE) indices have been evaluated. In the following, each of these indices is formulated [3,4,6,33].

$$LOEE = \sum_{t=1}^T [P_{LCB}(t) - P_{Inv-CB}(t)] \quad (14)$$

$$ENSP = \frac{LOEE}{\sum_{t=1}^T P_{LCB}(t)} \quad (15)$$

$$LOLE = \frac{\sum_{t=1}^T LOL}{T} \quad (16)$$

where $P_{LCB}(t)$ is the load demand of the residential complex at time t .

3.3. Constraints

In this study, the reliability criterion is presented as the maximum value of $ENSP$ ($ENSP_{max}$) as follows:

$$ENSP \leq ENSP_{max} \quad (17)$$

Also, the constraints of the system equipment are presented as follows:

$$N_{PV}^{\min} \leq N_{pv} \leq N_{PV}^{\max} \quad (18)$$

$$P_{El}^{\min} \leq P_{El} \leq P_{El}^{\max} \quad (19)$$

$$E_{HST}^{\min} \leq E_{HST} \leq E_{HST}^{\max} \quad (20)$$

$$P_{FC}^{\min} \leq P_{FC} \leq P_{FC}^{\max} \quad (21)$$

$$P_{Inv}^{\min} \leq P_{Inv} \leq P_{Inv}^{\max} \quad (22)$$

where N_{PV}^{\min} , P_{El}^{\min} , E_{HST}^{\min} , P_{FC}^{\min} , and P_{Inv}^{\min} are the minimum number of PVs, the minimum inverter power, the minimum energy of the hydrogen tank, the minimum fuel cell power, and the minimum transferred inverter power to the load, respectively. Also, N_{PV}^{\max} , P_{El}^{\max} , E_{HST}^{\max} , P_{FC}^{\max} , and P_{Inv}^{\max} are, respectively, the maximum number of PVs, the maximum inverter power, the maximum energy of the hydrogen tank, the maximum fuel cell power, and the maximum inverter-transferred power to the load.

4. Optimization Method

4.1. Overview of AEO

The AEO [30] includes three operators: production, consumption, and decomposition.

4.1.1. Production

In a productive ecosystem, food provides energy, along with carbon dioxide, water, sunlight, and nutrients created by decomposers. The generation operator assists the AEO [30] to randomly replace the previous one (x_n) with a new individual (x_{rand}). Production behaviour is defined below [30]:

$$x_1(t+1) = (1-a)x_{NP}(t) + ax_{rand}(t) \quad (23)$$

$$a = (1-t/T)r_1 \quad (24)$$

$$x_{rand} = r(U-L) + L \quad (25)$$

where NP represents the population size, T is the maximum number of iterations of the algorithm, L and U refer to the upper and lower boundaries of the search space.

4.1.2. Consumption

In the AEO [30], a simple and parameter-free random walk at a point based on the Levy flight, named the consumption factor, will be [30]:

$$C = \frac{1}{2} \frac{v_1}{|v_2|} \quad (26)$$

$$v_1 \sim N(0,1), \quad v_2 \sim N(0,1) \quad (27)$$

where $N(0,1)$ refers to the normal distribution with a zero mean and standard deviation.

Herbivore: The consumption pattern of vegetarians will be [30]:

$$x_i(t+1) = x_i(t) + C.(x_i(t) - x_1(t)), \quad i \in [2, \dots, n] \quad (28)$$

Carnivore: The consumption pattern of a carnivore can be modelled by Equation (29) [30]:

$$\begin{cases} x_i(t+1) = x_i(t) + C.(x_i(t) - x_1(t)), & i \in [2, \dots, NP] \\ j = randi([2 \quad i-1]) \end{cases} \quad (29)$$

Omnivore: If a consumer happens to be considered a consumer, it can consume both a consumer that has greater energy and a producer. This behaviour is defined here [30]:

$$\begin{cases} x_i(t+1) = x_i(t) + C.(x_i(t) - x_1(t)) + (1-r_2)(x_i(t) - x_j(t)), & i = 3, \dots, NP \\ j = randi([2 \quad i-1]) \end{cases} \quad (30)$$

r_2 represents a random number in the interval $[0, 1]$.

4.1.3. Decomposition

In the decomposition process, if an individual dies, the decomposer decomposes itself. The decomposition process is defined as follows [30]:

$$x_i(t+1) = x_n(t) + D.(e.x_n(t) - h.x_i(t)), \quad i = 1, \dots, NP \quad (31)$$

$$D = 3u, \quad u \sim N(0,1) \quad (32)$$

$$e = r_3.randi([1 \quad 2]) - 1 \quad (33)$$

$$h = 2.r_3 - 1 \quad (34)$$

4.2. Overview of IAEO

The lens imaging dynamic learning approach [31] is considered to prevent the AEO algorithm from getting trapped in the local optimum according to Figure 2. As you can see, on the left side of the y -axis, the person marked with F, its projection on the x -axis is shown with X, and its distance from the x -axis is marked with ζ . When passed through

a convex lens, F forms an inverse F' whose image on the x -axis is denoted by X' and its distance from the x -axis is defined as ξ' . Person X and person opposite X' are selected.

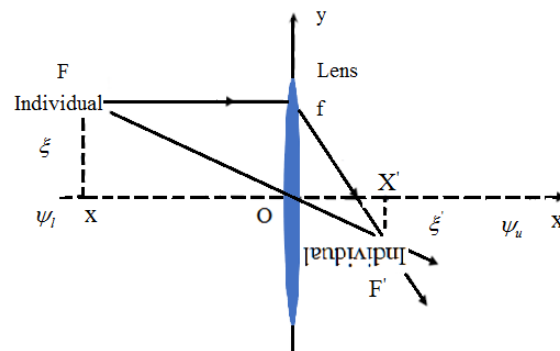


Figure 2. Strategy of dynamic lens-imaging learning.

X' is obtained as follows [31]:

$$X' = \frac{\psi_u + \psi_l}{2} + \frac{\psi_u + \psi_l}{2 \times \mu} - \frac{X}{\mu} \quad (35)$$

Scaling based on nonlinear dynamic reduction μ is defined as follows [31]:

$$\mu = \lambda^{\min} - (\lambda^{\max} - \lambda^{\min}) \times \left(\frac{t}{T}\right)^2 \quad (36)$$

where λ^{\max} and λ^{\min} represent the upper and lower scaling factors (100 and 10, respectively) [31]. Equation (35) is defined for n -dimensional space by [31]

$$X'_j = \frac{\psi_{uj} + \psi_{lj}}{2} + \frac{\psi_{uj} + \psi_{lj}}{2 \times \alpha} - \frac{X_j}{\alpha} \quad (37)$$

where X_j and X'_j refer to the X_0 and X components in dimension j ; and ψ_{lj} and ψ_{uj} , respectively, indicate the upper and lower limits of dimension j .

5. Implementation of the IAEO

The implementation steps of the IAEO in solving the HPV/FC energy system design problem are described below.

Step (1) *Application of HES data and algorithm.* In this step, the data set, such as weather data, technical and economical specifications, and algorithm data, are initiated.

Step (2) *Determining random variables per algorithm population.* In this stage, optimization parameters are found within the specified range for all populations randomly.

Step (3) *Calculate the objective function.* The objective function of TNPC (Equation (9)) is calculated considering the design constraints (Equations (17)–(22)) for each set of randomly chosen variables in step 2. After sorting, the set with the lowest TNPC (Equation (9)) will be assumed to be the best solution for this step.

Step (4) *Update the population of the algorithm.* At this stage, the population is updated.

Step (5) *Find the value of the objective function of the updated population.* The value of the TNPC cost function (Equation (9)) of the new set of variables from step 4 is calculated, and if it is better, it replaces the previous solution obtained in step 3.

Step (6) *Population update based on dynamic imaging-lens learning strategy.* In this step, the learning strategy of lens-dynamic imaging is implemented, the population is updated, and a set of new variables is selected.

Step (7) *Compute the objective function for the updated population based on the dynamic imaging-lens learning strategy.* At this stage, the TNPC is calculated for the set of new

variables, and if the obtained solution is better than the solution from step 5, it will be replaced.

Step (8) *Checking the convergence conditions*. In this step, the above steps are repeated until the convergence conditions are met. If there is convergence, jump to step 9; otherwise, return to step 4.

Step (9) *Stop the algorithm and save the best solution*. At this stage, when the algorithm reaches the convergence criterion, the algorithm is stopped, and the best variable set is saved.

6. Results and Discussion

6.1. Hybrid System Data

In this study, the design problem relies on practical data on the irradiance and ambient temperature for Kuala Lumpur (3.1569° N, 101.7123° E) in Malaysia [34,35]. The average monthly minimum and maximum radiation are reported in November and April, with values of 3.99 kW and 4.92 kW, respectively. The annual and hourly profiles of the irradiance and ambient temperature for Kuala Lumpur are shown in Figures 3 and 4, respectively [34,35]. In Figure 5, the load demand curve of the residential complex is presented with a peak load of 50 kW. In this study, the design of a hybrid system based on a fuel cell has been implemented based on Ref. [15].

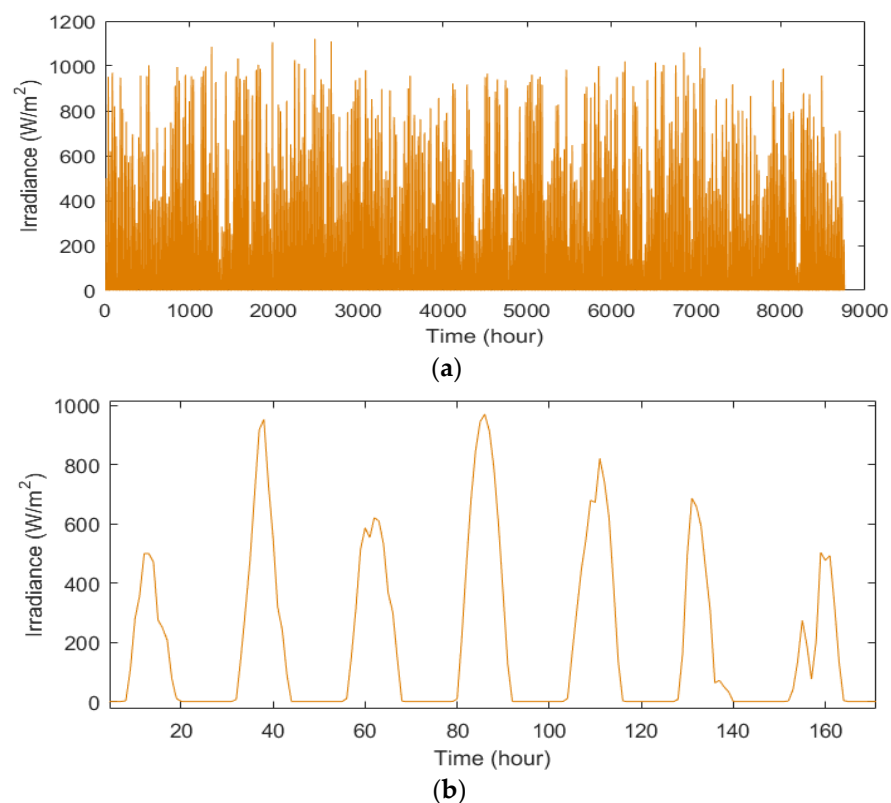


Figure 3. Irradiance of Kuala Lumpur during (a) a year and (b) a week.

6.2. Sizing Results for $ENSP_{max} = 1\%$

In this section, the optimal design of the HPV/FC system to minimise the TNPC and meet the demand of a residential complex is presented using the IAEO, considering $ENSP_{max} = 1\%$. Figure 6 shows the convergence process of each meta-heuristic algorithm in solving the design problem. The numerical results of the optimal design of an HPV/FC system considering $ENSP_{max} = 1\%$, are given in Tables 2–4. According to the obtained results, it is clear that the IAEO, by determining the optimal capacity of the equipment, has obtained a lower value of TNPC and COE compared to other methods.

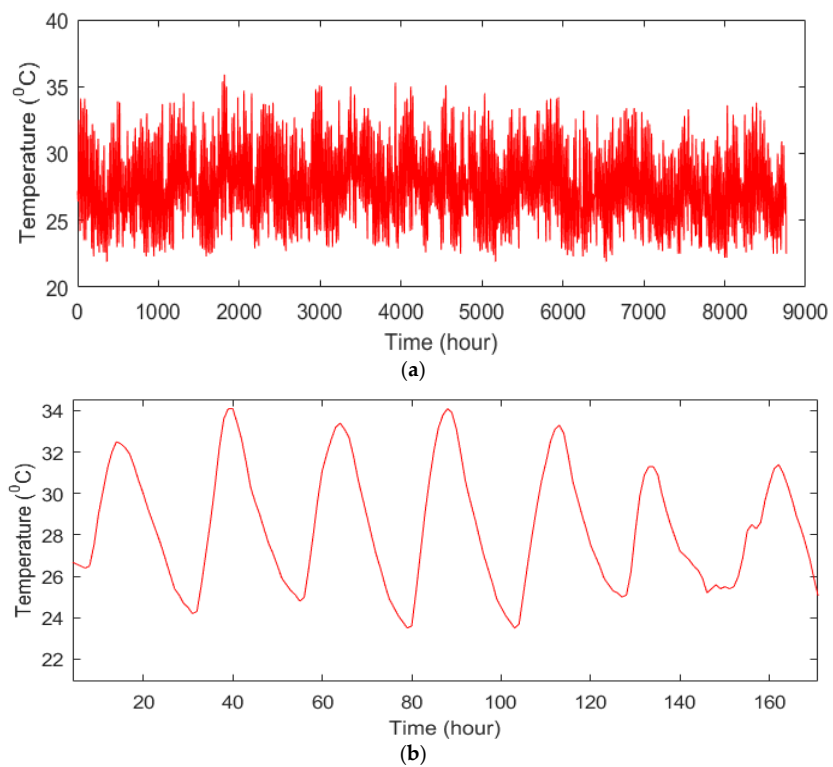


Figure 4. Temperature of Kuala Lumpur during (a) a year and (b) a week.

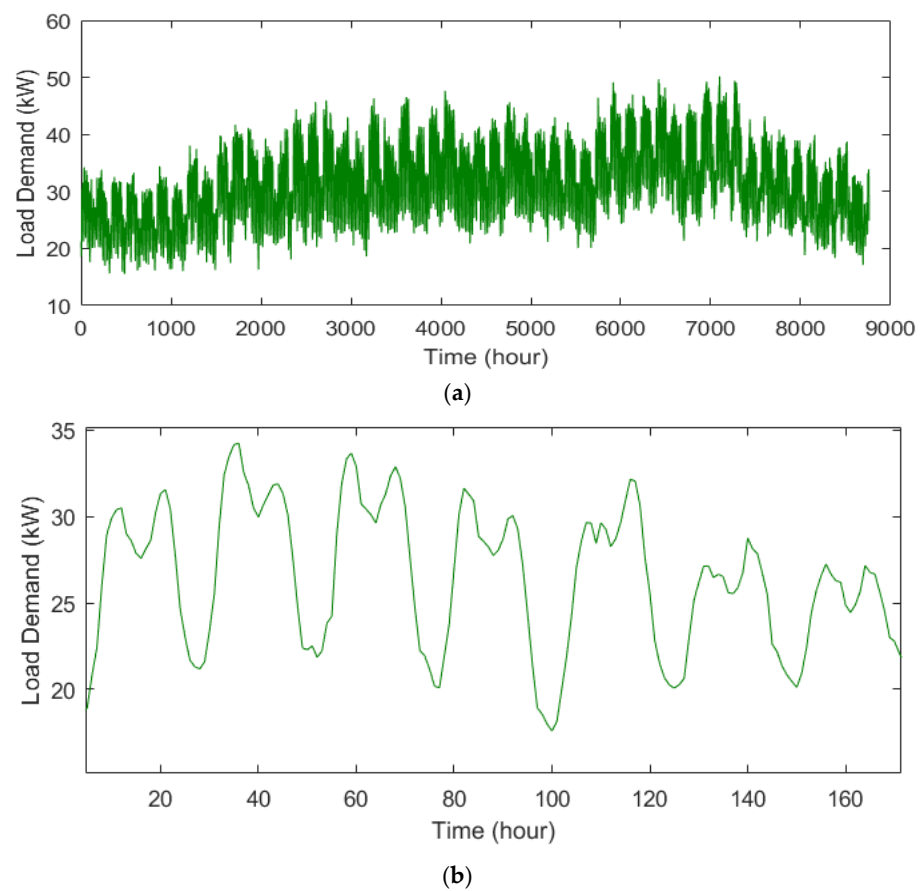


Figure 5. Annual load demand curve of the residential complex during (a) a year and (b) a week.

Table 1 reports the technical and economic specifications of the HES equipment.

Table 1. Techno-economic data of the PV/FC energy system [15,36].

Component	CC (US\$/Unit)	RC (US\$/Unit)	OM (US\$/Unit-yrs.)	Rated Size	Efficiency (%)	Lifetime (yr)
PV	2000	1700	100	1 kW	-	20
EL	2000	1500	25	1 kW	75	20
HST	1300	1200	15	1 kg	95	20
FC	4000	3500	200	1 kW	50	5
Inverter	800	750	7	1 kW	95	10

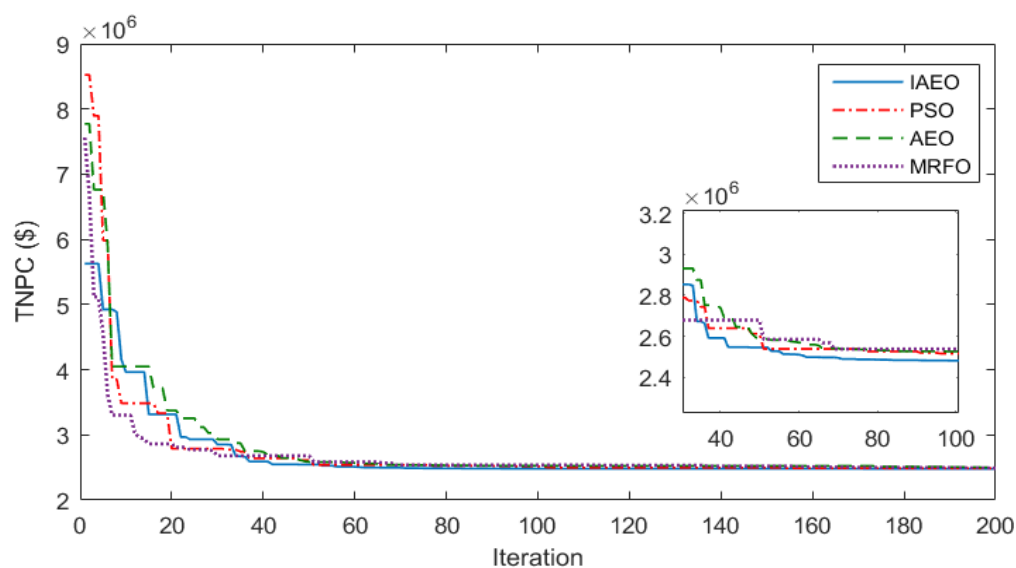


Figure 6. Convergence process of different algorithms in the sizing of HPV/FC energy systems considering $ENSP_{max} = 1\%$.

Table 2. Sizing results of the HPV/FC energy system considering $ENSP_{max} = 1\%$.

Algorithm/Item	N_{PV} (kW)	P_{EL} (kW)	M_{HST} (kg)	P_{FC} (kW)	P_{Inv} (kW)
IAEO	471.44	171.33	98.38	47.88	50.18
AEO	480.59	168.12	96.88	47.16	50.02
PSO	474.02	169.60	100.04	47.89	50.15
MRFO	475.94	168.09	99.94	47.86	50.11

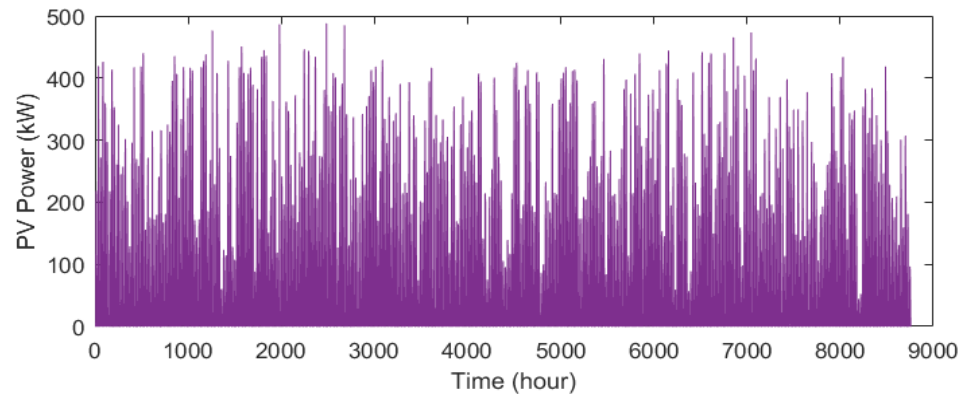
Table 3. Statistical analysis for different algorithms in the sizing of the HPV/FC energy system considering $ENSP_{max} = 1\%$.

Algorithm/Item	Best (M\$)	Mean (M\$)	Worst (M\$)	Std (M\$)
IAEO	2.480	2.491	2.498	0.0067
AEO	2.500	2.512	2.524	0.0104
PSO	2.487	2.496	2.503	0.0069
MRFO	2.490	2.505	2.514	0.0078

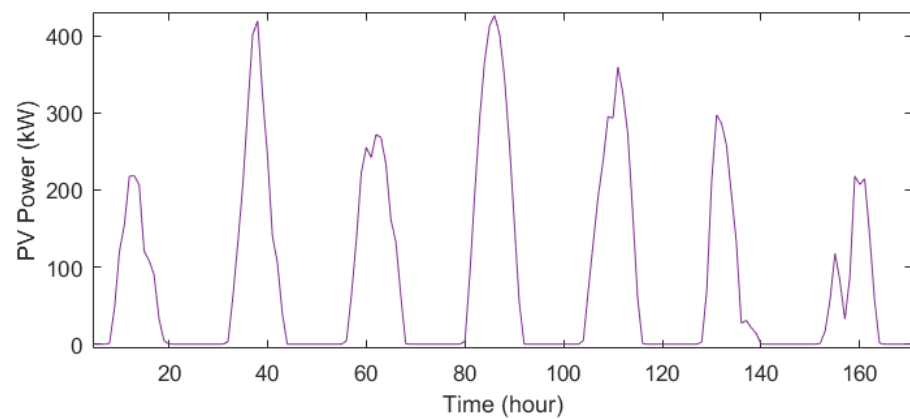
In Figures 7–10, the annual curve of the PV power production, energy stored in the hydrogen tank, transmission power of PV sources to the inverter, and FC production power are shown, respectively. In Figure 11, the ENSP curve is also shown during one year, which shows that most of the unsupplied energy of the system is related to the hours of 6500 to 7800.

Table 4. Reliability and cost results of HPV/FC energy systems considering $ENSP_{max} = 1\%$.

Algorithm/Item	ENSP (%)	LOLE (h/yr)	LOEE (MWh/yr)	TNPC (M\$)	COE (\$/kWh)
IAEO	0.0058	82	0.1612	2.480	0.4465
AEO	0.0072	89	0.1999	2.500	0.4501
PSO	0.0060	86	0.1666	2.487	0.4478
MRFO	0.0071	87	0.1971	2.490	0.4483



(a)



(b)

Figure 7. Generated power from PV resources considered in the sizing of the HPV/FC energy system via the IAEO, considering $ENSP_{max} = 1\%$ during (a) a year and (b) a week.

6.3. Sizing Results for $ENSP_{max} = 5\%$

The results related to the optimal design of the HPV/FC energy system are presented using the IAEO for $ENSP_{max} = 5\%$. The convergence trend for various algorithms in achieving the optimal design solution is drawn in Figure 12, where the comparison of the convergence process of the algorithms shows the superiority of the IAEO method in finding the best solution.

The results of the HPV/FC energy system design for $ENSP_{max} = 5\%$ are presented in Tables 5–7. The TNPC values obtained by the IAEO, AEO, PSO, and MRFO algorithms are USD 2.247 M, USD 2.358 M, USD 2.249 M, and USD 2.251 M, respectively, and the COE values for each kWh supply are USD 0.4046, USD 0.4242, USD 0.4049, and USD 0.4053, respectively. According to the obtained results, the IAEO obtained a lower value for TNPC and COE compared to other methods.

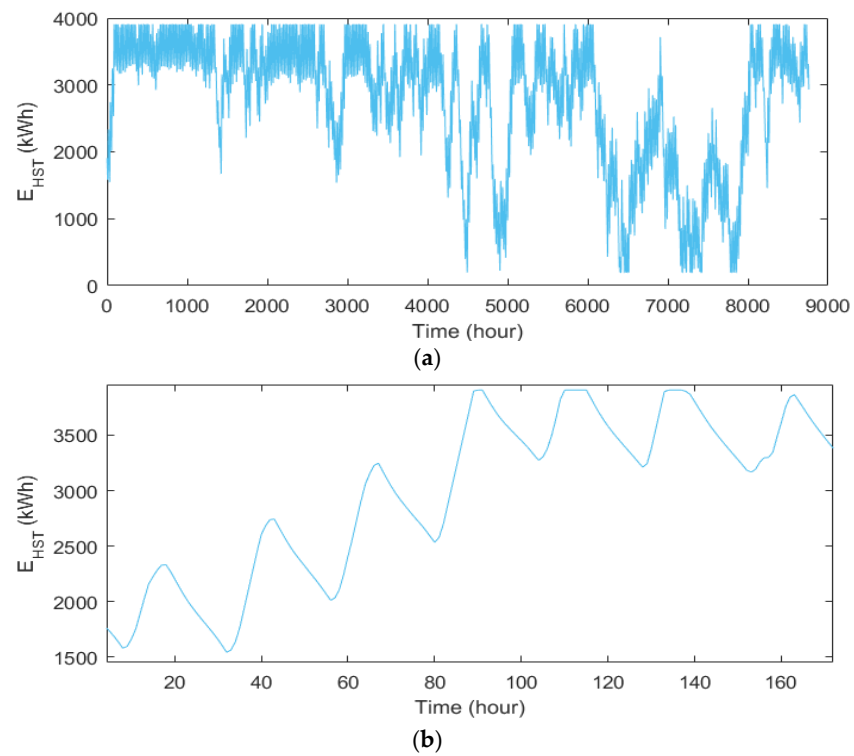


Figure 8. Hydrogen storage tank energy considered in the sizing of the HPV/FC energy system via the IAEO, considering $ENSP_{max} = 1\%$ during (a) a year and (b) a week.

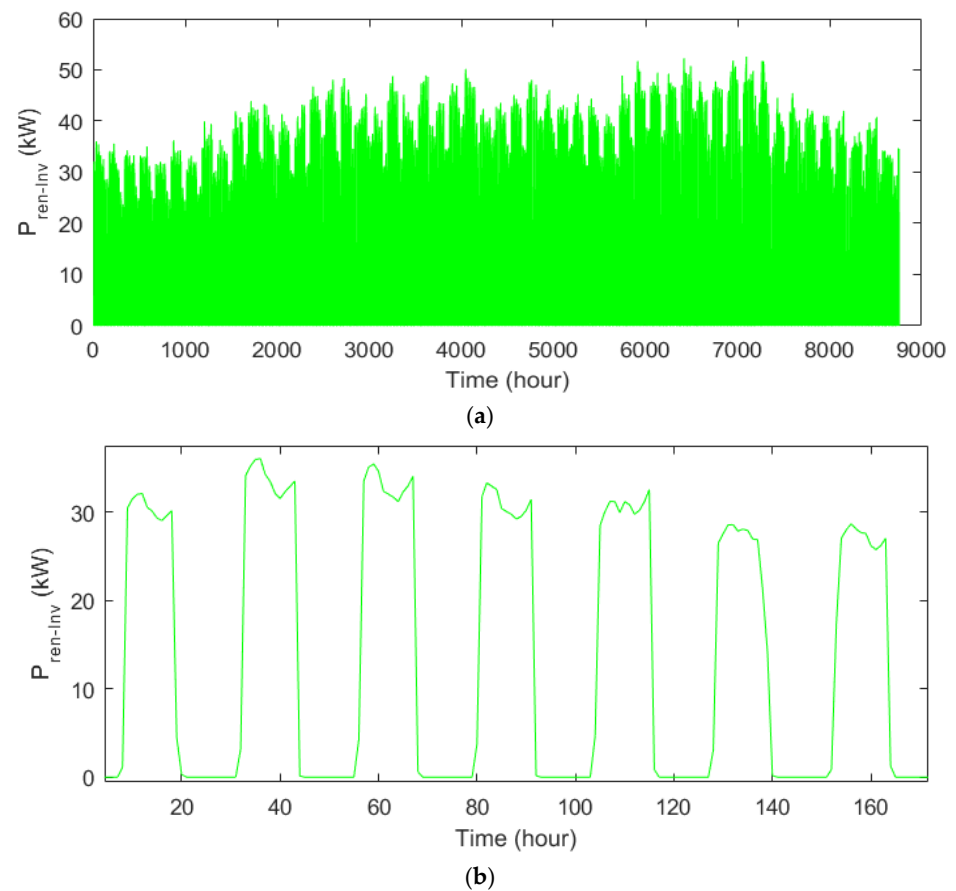


Figure 9. Delivered power to the inverter by the PV resources considered in the sizing of the HPV/FC energy system via the IAEO, considering $ENSP_{max} = 1\%$ during (a) a year and (b) a week.

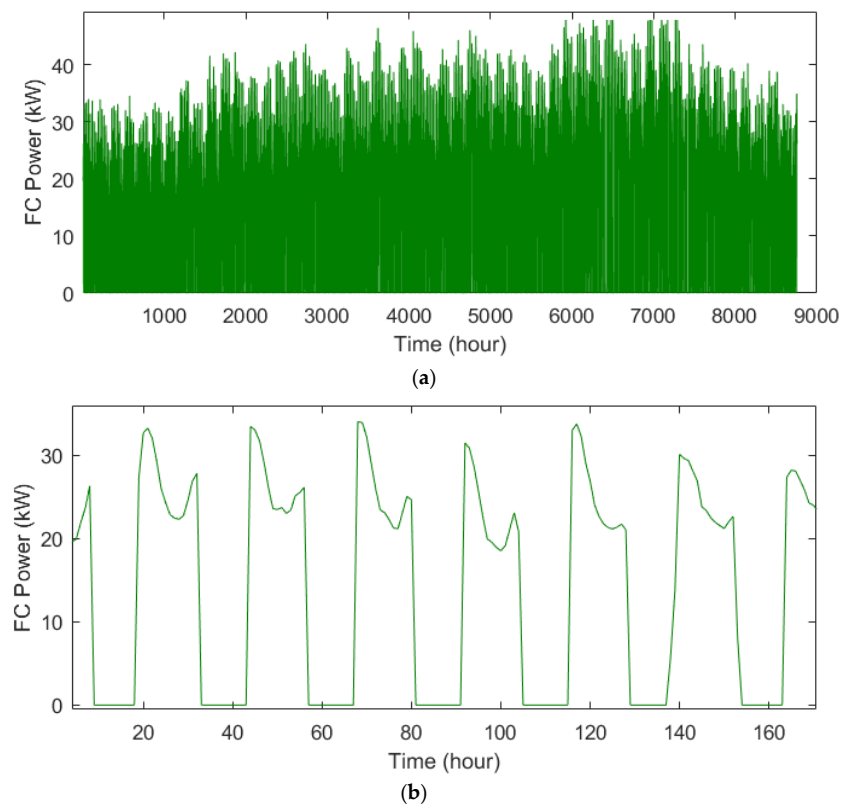


Figure 10. FC power in the sizing of the HPV/FC energy system via the IAEO, considering $ENSP_{\max} = 1\%$ during (a) a year and (b) a week.

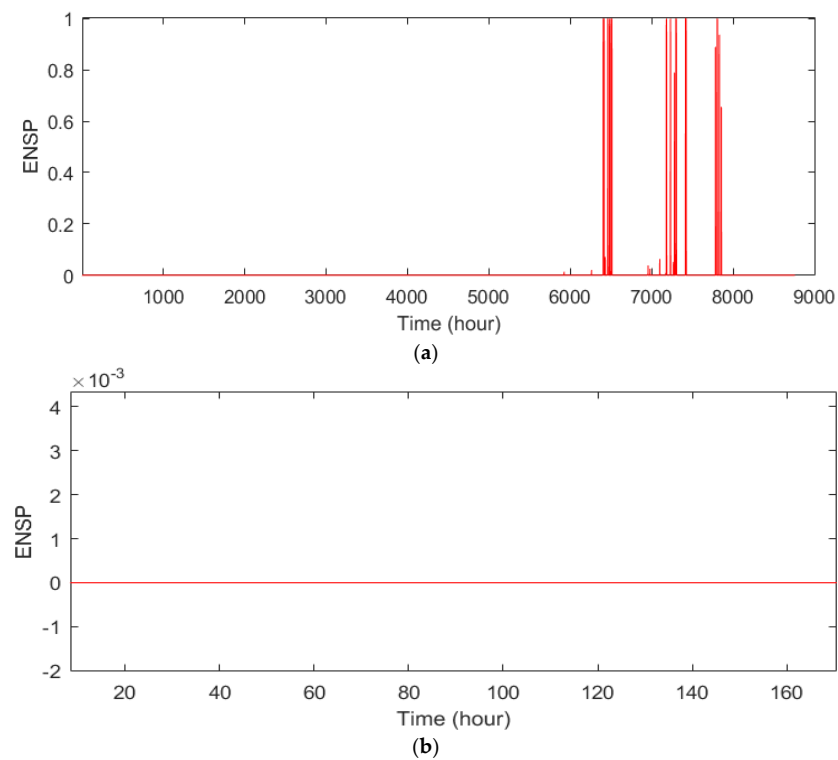


Figure 11. ENSP in the sizing of the HPV/FC energy system via the IAEO, considering $ENSP_{\max} = 1\%$ during (a) a year and (b) a week.

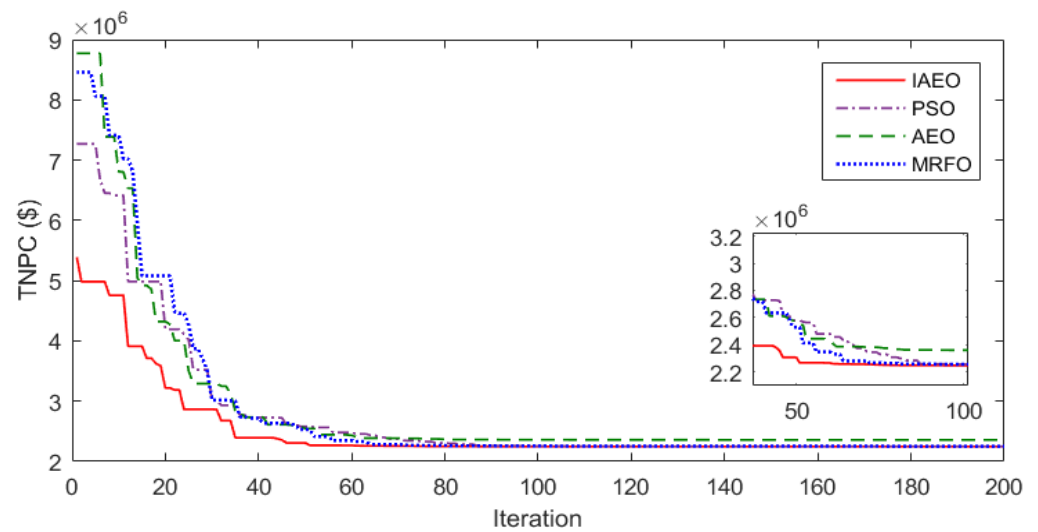


Figure 12. Convergence process of different algorithms in the sizing of the HPV/FC energy system considering an $ENSP_{max}$ of 5%.

Table 5. Results related to scaling the HPV/FC energy system considering $ENSP_{max} = 5\%$.

Algorithm/Item	N_{PV} (kW)	P_{EL} (kW)	M_{HST} (kg)	P_{FC} (kW)	P_{Inv} (kW)
IAEO	439.58	147.99	81.74	42.26	49.44
AEO	419.31	153.54	108.61	52.86	48.93
PSO	430.16	154.74	91.11	42.20	49.40
MRFO	443.67	148.98	75.30	41.92	49.35

Table 6. Statistical analysis for different algorithms in the sizing of the HPV/FC energy system considering $ENSP_{max} = 5\%$.

Algorithm/Item	Best (M\$)	Mean (M\$)	Worst (M\$)	Std (M\$)
IAEO	2.247	2.252	2.257	0.0048
AEO	2.258	2.266	2.274	0.0077
PSO	2.249	2.257	2.263	0.0054
MRFO	2.251	2.263	2.270	0.0065

Table 7. Reliability and cost results of the HPV/FC energy system considering $ENSP_{max} = 5\%$.

Algorithm/Item	$ENSP$ (%)	LOLE (h/yr)	LOEE (MWh/yr)	TNPC (M\$)	COE (\$/kWh)
IAEO	0.0289	408	0.7925	2.247	0.4046
AEO	0.0336	438	0.9325	2.258	0.4242
PSO	0.0291	426	0.7928	2.249	0.4049
MRFO	0.0294	429	0.7435	2.251	0.4053

In Figures 13–16, PV power generation, hydrogen tank energy, PV power transmission to the inverter, and FC power are depicted. In Figure 17, the annual changes of the $ENSP$ presented indicate that the most not-supplied energy is related to the hours 7800 to 4500.

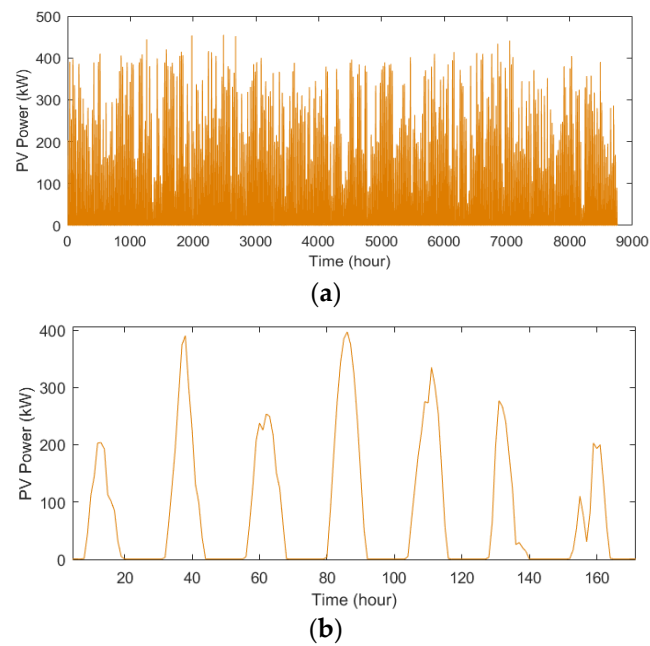


Figure 13. Generated power by PV resources in the sizing of the HPV/FC energy system via the IAEO, considering $ENSP_{\max} = 5\%$ during (a) a year and (b) a week.

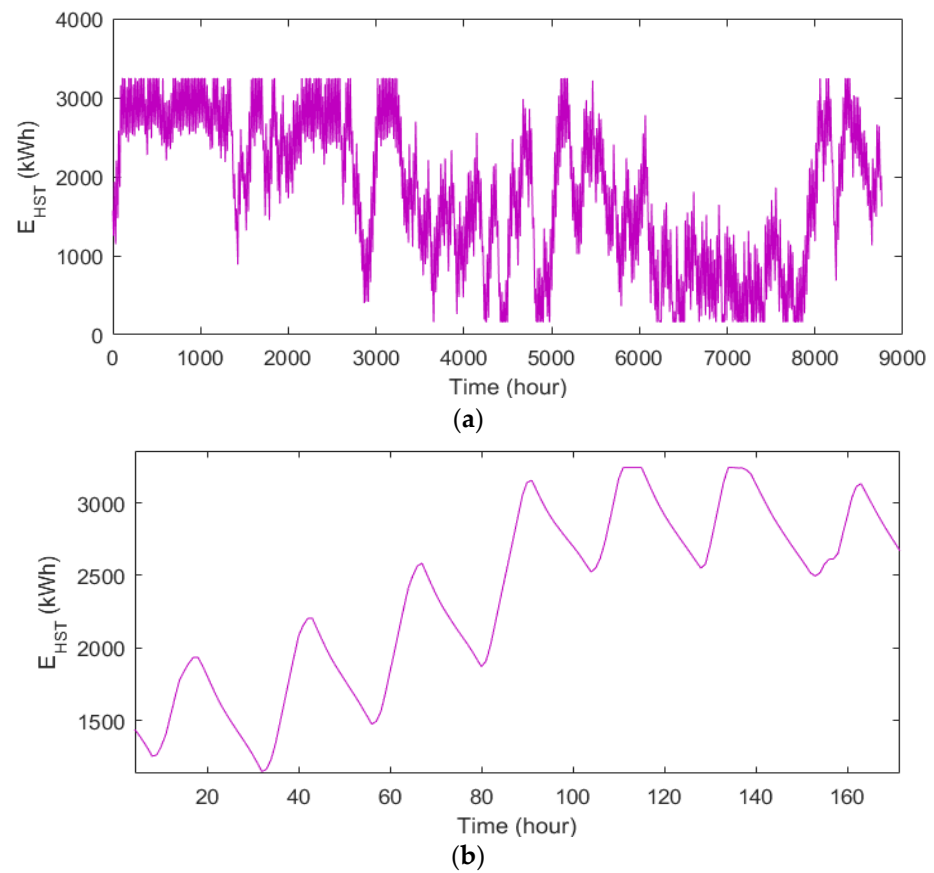


Figure 14. Hydrogen storage tank energy considered in the sizing of the HPV/FC energy system via the IAEO, considering $ENSP_{\max} = 5\%$ during (a) a year and (b) a week.

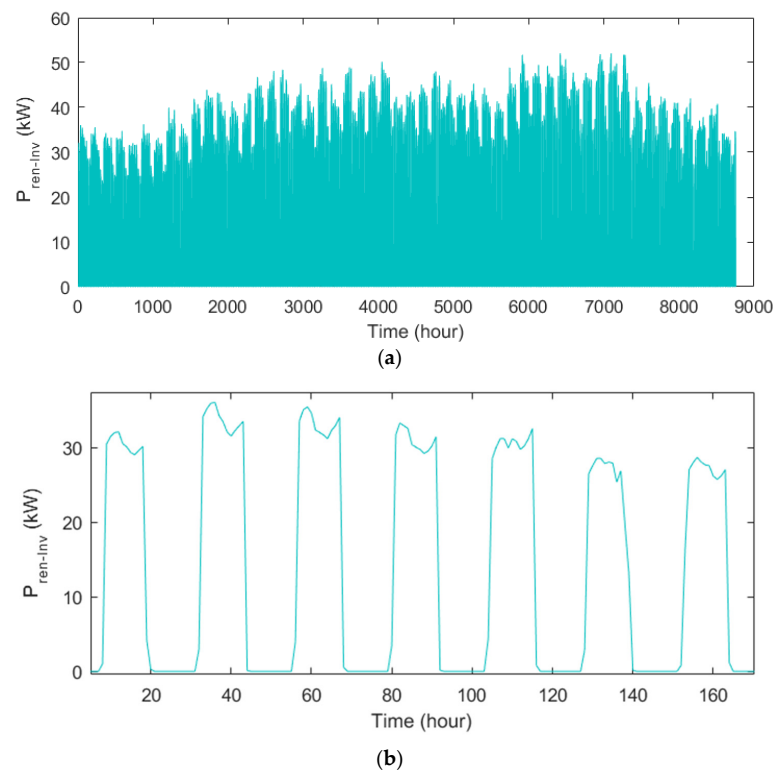


Figure 15. Delivered power to the inverter by the PV resources in the sizing of the HPV/FC energy system via the IAEO, considering $ENSP_{max} = 5\%$ during (a) a year and (b) a week.

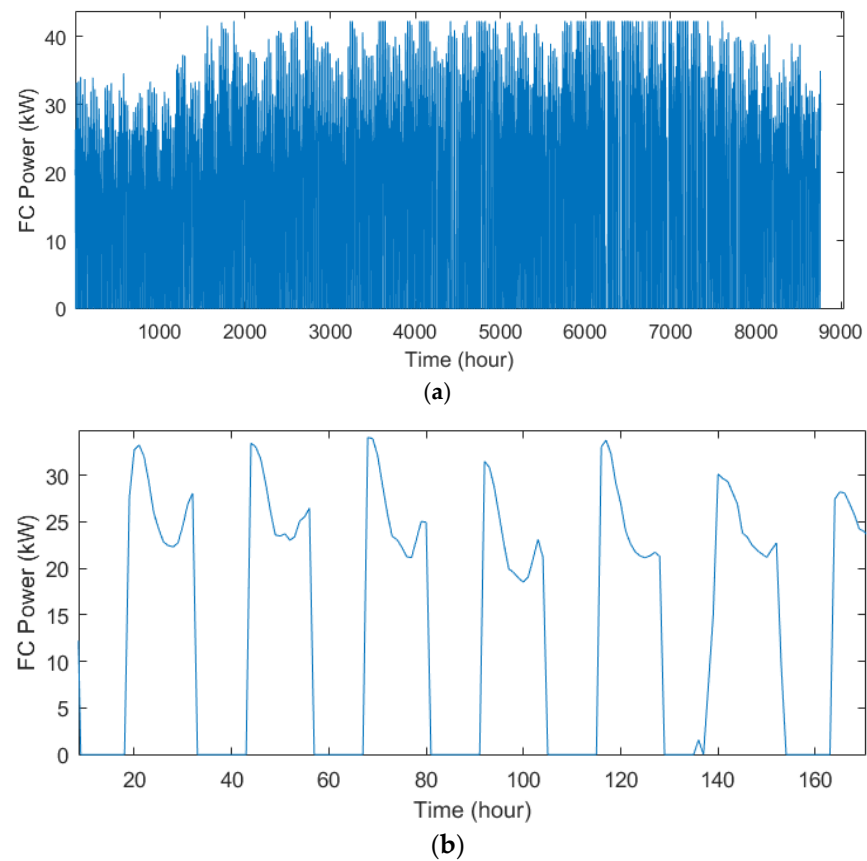


Figure 16. FC power in the sizing of the HPV/FC energy system via the IAEO, considering $ENSP_{max} = 5\%$ during (a) a year and (b) a week.

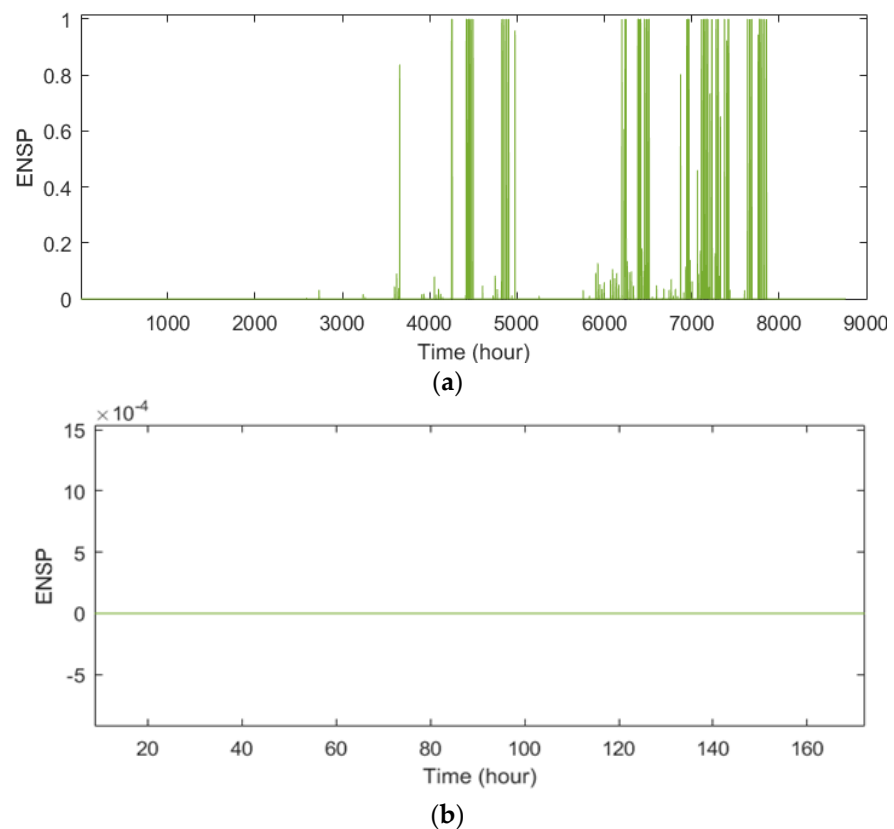


Figure 17. ENSP in the sizing of the HPV/FC energy system via the IAEO, considering $ENSP_{\max} = 5\%$ during (a) a year and (b) a week.

6.4. Results Comparison

In Sections 6.2 and 6.3, the results of the HPV/FC energy system design for $ENSP_{\max} = 1\%$ and 5% are presented using the IAEO. The convergence curve obtained from the implementation of the design problem for $ENSP_{\max}$ values equal to 1%, 5%, 10%, 15%, 20%, 25%, and 30% is presented in Figure 18, which shows the convergence process of the IAEO in reaching the best solution for different $ENSP_{\max}$ values. According to Tables 8 and 9, with the increase of the $ENSP_{\max}$ value, the values of the ENSP and LOEE increased, and vice versa. Also, with the increase in $ENSP_{\max}$, the TNPC and COE decreased, and vice versa.

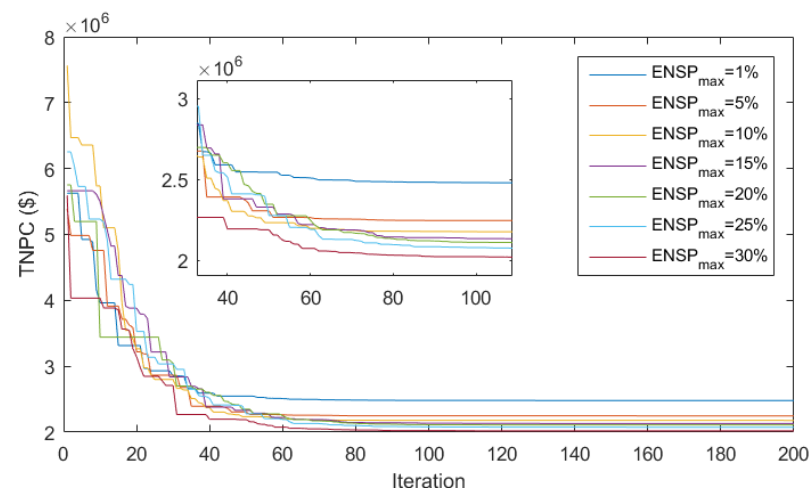


Figure 18. Convergence process of the IAEO in the sizing of HPV/FC energy systems, considering different $ENSP_{\max}$.

Table 8. Sizing results of HPV/FC energy systems using the IAEO, considering different $ENSP_{max}$.

$ENSP_{max}/Item$	N_{PV} (kW)	P_{EL} (kW)	M_{HST} (kg)	P_{FC} (kW)	P_{Inv} (kW)
1%	471.44	171.33	98.38	47.88	50.18
5%	439.58	147.99	81.74	42.26	49.44
10%	431.85	140.78	97.84	37.56	49.41
15%	429.90	144.15	94.66	33.77	48.65
20%	423.64	155.33	92.08	31.45	48.29
25%	413.88	131.82	88.54	29.99	47.68
30%	418.65	136.16	93.52	28.36	47.34

Table 9. Reliability and cost results in sizing HPV/FC energy systems using the IAEO, considering different $ENSP_{max}$.

$ENSP_{max}/Item$	$ENSP$ (%)	$LOLE$ (h/yr)	$LOEE$ (MWh/yr)	$TNPC$ (M\$)	COE (\$/kWh)
1%	0.0074	87	0.20599	2.480	0.4465
5%	0.0289	408	0.7925	2.247	0.4046
10%	0.0363	876	1.0091	2.178	0.3921
15%	0.0384	1314	1.0654	2.132	0.3838
20%	0.0417	1752	1.1578	2.109	0.3797
25%	0.0520	2117	1.4450	2.073	0.3732
30%	0.0614	2828	1.7062	2.018	0.3633

6.5. Sensitivity Analysis

6.5.1. Effect of HST Efficiency

The results of the hydrogen tank efficiency changes effect on the design problem using the IAEO, considering $ENSP_{max} = 5\%$, are presented in Table 1. Based on Tables 10 and 11, it has been observed that by increasing the efficiency of the hydrogen tank, the amount of $ENSP$ has decreased; in other words, the load reliability has increased, and the costs of the system, including $TNPC$ and COE , have decreased, and vice versa.

Table 10. Sizing results of an HPV/FC energy system using the IAEO and $ENSP_{max} = 5\%$ considering different HST efficiency values.

HST Efficiency/Item	N_{PV} (kW)	P_{EL} (kW)	M_{HST} (kg)	P_{FC} (kW)	P_{Inv} (kW)
80%	445.76	139.58	79.28	37.01	49.16
85%	477.62	160.12	88.91	42.22	50.20
90%	461.59	151.16	81.21	42.30	49.61
95%	439.58	147.99	81.74	42.26	49.44
100%	423.64	155.33	92.08	31.45	48.29

Table 11. Reliability and cost results in the sizing of HPV/FC energy systems using the IAEO and $ENSP_{max} = 5\%$ considering different HST efficiency values.

HST Efficiency/Item	$ENSP$ (%)	$LOLE$ (h/yr)	$LOEE$ (MWh/yr)	$TNPC$ (M\$)	COE (\$/kWh)
80%	0.0324	438	0.8997	2.483	0.4470
85%	0.0312	426	0.8663	2.395	0.4312
90%	0.0299	414	0.8302	2.318	0.4173
95%	0.0289	408	0.7925	2.247	0.4046
100%	0.0278	395	0.7719	2.185	0.3934

6.5.2. Effect of Load Variation

The results of the residential complex load demand changes are given in the design problem using the IAEO, considering $ENSP_{max} = 5\%$, in Table 1. Based on Tables 12 and 13, it is clear that with the increase in the load of the residential complex, the level of hydrogen production and storage, besides the production of fuel cell power, increases, and thus, TNPC and COE rise, and vice versa.

Table 12. Sizing results of an HPV/FC energy system using the IAEO and $ENSP_{max} = 5\%$ considering load variations.

$ENSP_{max}/Item$	N_{PV} (kW)	P_{EL} (kW)	M_{HST} (kg)	P_{FC} (kW)	P_{Inv} (kW)
60%* P_{Load}	258.36	91.00	55.70	25.55	30.13
80%* P_{Load}	341.62	119.91	79.46	34.42	40.15
100%* P_{Load}	439.58	147.99	81.74	42.26	49.44
120%* P_{Load}	546.75	164.92	82.35	50.99	60.34
140%* P_{Load}	610.44	204.36	122.92	59.85	70.25

Table 13. Reliability and cost results in sizing the HPV/FC energy system using the IAEO and $ENSP_{max} = 5\%$ considering load variations.

$ENSP_{max}/Item$	ENSP (%)	LOLE (h/yr)	LOEE (MWh/yr)	TNPC (M\$)	COE (\$/kWh)
60%* P_{Load}	0.0200	302	0.3340	1.349	0.2428
80%* P_{Load}	0.0224	375	0.4979	1.799	0.3239
100%* P_{Load}	0.0289	408	0.7925	2.247	0.4046
120%* P_{Load}	0.0295	523	0.9838	2.705	0.4870
140%* P_{Load}	0.0309	619	1.2022	3.147	0.5666

6.6. Comparisons

The results obtained from the optimal configuration of the HPV/FC energy system using IAEO for $ENSP_{max} = 5\%$ are compared with previous studies, and the report is listed in Table 14. Ref. [37] presents a comparative design study for the HPV/FC system using the whale optimization algorithm to minimise the energy cost, while meeting the reliability limits. Accordingly, the energy cost for supplying 1 kW of load demand in Kuala Lumpur is much lower than supplying it in Ref. [37].

Table 14. Results of comparisons.

Ref.	Hybrid System	Region	Reliability Constraint	COE (\$/kWh)
This paper	PV/FC	Kuala Lumpur/Malaysia	1%	0.4465
This paper	PV/FC	Kuala Lumpur/Malaysia	5%	0.4046
[37]	PV/FC	Gorgan/Iran	1%	1.7924
[37]	PV/FC	Urmia/Iran	1%	2.0893
[37]	PV/FC	Yazd/Iran	1%	0.8968

7. Conclusions

In this study, an HPV/FC system based on hydrogen storage was designed to cover the annual complex load considering the meteorological data of Kuala Lumpur, Malaysia, using the IAEO. The results showed that the proposed design methodology based on the IAEO was able to obtain the optimal combination of the system, with a lower cost and a higher level of reliability compared to the conventional AEO, PSO, and MRFO algorithms, which shows the effectiveness of the dynamic lens-imaging learning strategy in the improved algorithm. Also, the results showed that the increase (decrease) of the reliability constraint by reducing (increasing) the level of production and storage has reduced (increased) the

design costs. In addition, the results show that the use of inverters and hydrogen tanks with higher efficiency has reduced design costs due to better power transmission by the inverter and increased storage capacity by the tank. The design of a hybrid photovoltaic/fuel cell system considering the uncertainty of production and load consumption is proposed for future work.

Author Contributions: J.Y. and Y.-L.C. carried out the exploration of ideas and conducted a review of systems and methods. They contributed to the survey studies and methods and came up with the presented ideas, while also writing the manuscript with the support of P.L.Y., C.S.K. and Y.-L.C. These individuals provided suggestions on the experimental setup and analytical results. Y.-L.C. and P.L.Y. also offered their insights on the research ideas and analytical results and assisted in the writing of the manuscript. Funding support was provided by Y.-L.C., who also co-wrote the manuscript. M.B. contributed to the implementation of the mathematical optimization algorithm and to the statistical analysis. All authors have read and agreed to the published version of the manuscript.

Funding: This work was also funded by the National Science and Technology Council in Taiwan, under grant numbers NSTC-109-2628-E-027-004-MY3, NSTC-111-2218-E-027-003, and NSTC-111-2622-8-027-009, and was also supported by the Ministry of Education of Taiwan under Official Document No. 1112303249, entitled “The study of artificial intelligence and advanced semi-conductor manufacturing for female STEM talent education and industry–university value-added cooperation promotion”.

Institutional Review Board Statement: Not applicable.

Informed Consent Statement: Not applicable.

Data Availability Statement: Not applicable.

Conflicts of Interest: The authors declare no conflict of interest.

References

1. Alanazi, A.; Alanazi, M.; Nowdeh, S.A.; Abdelaziz, A.Y.; Abu-Siada, A. Stochastic-Metaheuristic Model for Multi-Criteria Allocation of Wind Energy Resources in Distribution Network Using Improved Equilibrium Optimization Algorithm. *Electronics* **2022**, *11*, 3285. [[CrossRef](#)]
2. Alanazi, A.; Alanazi, M.; Nowdeh, S.A.; Abdelaziz, A.Y.; El-Shahat, A. An optimal sizing framework for autonomous photovoltaic/hydrokinetic/hydrogen energy system considering cost, reliability and forced outage rate using horse herd optimization. *Energy Rep.* **2022**, *8*, 7154–7175. [[CrossRef](#)]
3. Naderipour, A.; Kamyab, H.; Klemeš, J.J.; Ebrahimi, R.; Chelliapan, S.; Nowdeh, S.A.; Abdullah, A.; Marzbali, M.H. Optimal design of hybrid grid-connected photovoltaic/wind/battery sustainable energy system improving reliability, cost and emission. *Energy* **2022**, *257*, 124679. [[CrossRef](#)]
4. Naderipour, A.; Abdul-Malek, Z.; Vahid, M.Z.; Seifabad, Z.M.; Hajivand, M.; Arabi-Nowdeh, S. Optimal, Reliable and Cost-Effective Framework of Photovoltaic-Wind-Battery Energy System Design Considering Outage Concept Using Grey Wolf Optimizer Algorithm—Case Study for Iran. *IEEE Access* **2019**, *7*, 182611–182623. [[CrossRef](#)]
5. Qi, X.; Wang, J.; Królczyk, G.; Gardoni, P.; Li, Z. Sustainability analysis of a hybrid renewable power system with battery storage for islands application. *J. Energy Storage* **2022**, *50*, 104682. [[CrossRef](#)]
6. Moghaddam, M.J.H.; Kalam, A.; Nowdeh, S.A.; Ahmadi, A.; Babanezhad, M.; Saha, S. Optimal sizing and energy management of stand-alone hybrid photovoltaic/wind system based on hydrogen storage considering LOEE and LOLE reliability indices using flower pollination algorithm. *Renew. Energy* **2018**, *135*, 1412–1434. [[CrossRef](#)]
7. Kaviani, A.K.; Riahy, G.H.; Kouhsari, S.H.M. Optimal design of a reliable hydrogen-based stand-alone wind/PV generating system, considering component outages. *Renew. Energy* **2009**, *34*, 2380–2390. [[CrossRef](#)]
8. Hoseinzadeh, S.; Garcia, D.A. Techno-economic assessment of hybrid energy flexibility systems for islands’ decarbonization: A case study in Italy. *Sustain. Energy Technol. Assess.* **2021**, *51*, 101929. [[CrossRef](#)]
9. Hassan, Q.; Jaszczur, M.; Hafedh, S.A.; Abbas, M.K.; Abdulateef, A.M.; Hasan, A.; Abdulateef, J.; Mohamad, A. Optimizing a microgrid photovoltaic-fuel cell energy system at the highest renewable fraction. *Int. J. Hydrog. Energy* **2022**, *47*, 13710–13731. [[CrossRef](#)]
10. Bouaouda, A.; Sayouti, Y. Hybrid Meta-Heuristic Algorithms for Optimal Sizing of Hybrid Renewable Energy System: A Review of the State-of-the-Art. *Arch. Comput. Methods Eng.* **2022**, *29*, 4049–4083. [[CrossRef](#)]
11. Al-Othman, A.; Tawalbeh, M.; Martis, R.; Dhou, S.; Orhan, M.; Qasim, M.; Olabi, A.G. Artificial intelligence and numerical models in hybrid renewable energy systems with fuel cells: Advances and prospects. *Energy Convers. Manag.* **2022**, *253*, 115154. [[CrossRef](#)]
12. Sanajaoba, S. Optimal sizing of off-grid hybrid energy system based on minimum cost of energy and reliability criteria using firefly algorithm. *Sol. Energy* **2019**, *188*, 655–666. [[CrossRef](#)]

13. Ghorbani, N.; Kasaeian, A.; Toopshekan, A.; Bahrami, L.; Maghami, A. Optimizing a hybrid wind-PV-battery system using GA-PSO and MOPSO for reducing cost and increasing reliability. *Energy* **2018**, *154*, 581–591. [CrossRef]
14. Fodhil, F.; Hamidat, A.; Nadjemi, O. Potential, optimization and sensitivity analysis of photovoltaic-diesel-battery hybrid energy system for rural electrification in Algeria. *Energy* **2019**, *169*, 613–624. [CrossRef]
15. Jahannoosh, M.; Nowdeh, S.A.; Naderipour, A.; Kamyab, H.; Davoodkhani, I.F.; Klemeš, J.J. New Hybrid Meta-Heuristic Algorithm for Reliable and Cost-Effective Designing of Photovoltaic/Wind/Fuel Cell Energy System Considering Load Interruption Probability. *J. Clean. Prod.* **2020**, *278*, 123406. [CrossRef]
16. Das, B.K.; Alotaibi, M.A.; Das, P.; Islam, M.; Das, S.K.; Hossain, A. Feasibility and techno-economic analysis of stand-alone and grid-connected PV/Wind/Diesel/Batt hybrid energy system: A case study. *Energy Strat. Rev.* **2021**, *37*, 100673. [CrossRef]
17. Sun, H.; Ebadi, A.G.; Toughani, M.; Nowdeh, S.A.; Naderipour, A.; Abdullah, A. Designing framework of hybrid photovoltaic-biowaste energy system with hydrogen storage considering economic and technical indices using whale optimization algorithm. *Energy* **2021**, *238*, 121555. [CrossRef]
18. Bouchekara, H.R.; Shahriar, M.; Irshad, U.; Aban, Y.S.; Mahmud, M.P.; Javaid, M.; Ramli, M.A.; Farjana, S.H. Optimal sizing of hybrid photovoltaic/diesel/battery nanogrid using a parallel multiobjective PSO-based approach: Application to desert camping in Hafr Al-Batin city in Saudi Arabia. *Energy Rep.* **2021**, *7*, 4360–4375. [CrossRef]
19. Mohammed, A.Q.; Al-Anbari, K.A.; Hannun, R.M. Optimal Combination and Sizing of a Stand-Alone Hybrid Energy System Using a Nomadic People Optimizer. *IEEE Access* **2020**, *8*, 200518–200540. [CrossRef]
20. Guo, X.; Zhou, L.; Guo, Q.; Rouyendegh, B.D. An optimal size selection of hybrid renewable energy system based on Fractional-Order Neural Network Algorithm: A case study. *Energy Rep.* **2021**, *7*, 7261–7272. [CrossRef]
21. Mahmoud, F.S.; Diab, A.A.Z.; Ali, Z.M.; El-Sayed, A.-H.M.; Alquthami, T.; Ahmed, M.; Ramadan, H.A. Optimal sizing of smart hybrid renewable energy system using different optimization algorithms. *Energy Rep.* **2022**, *8*, 4935–4956. [CrossRef]
22. Naderipour, A.; Ramtin, A.R.; Abdullah, A.; Marzbali, M.H.; Nowdeh, S.A.; Kamyab, H. Hybrid energy system optimization with battery storage for remote area application considering loss of energy probability and economic analysis. *Energy* **2021**, *239*, 122303. [CrossRef]
23. Ghaffari, A.; Askarzadeh, A. Design optimization of a hybrid system subject to reliability level and renewable energy penetration. *Energy* **2020**, *193*, 116754. [CrossRef]
24. Cao, Y.; Yao, H.; Wang, Z.; Jermisittiparsert, K.; Yousefi, N. Optimal Designing and Synthesis of a Hybrid PV/Fuel cell/Wind System using Meta-heuristics. *Energy Rep.* **2020**, *6*, 1353–1362. [CrossRef]
25. Singh, S.; Chauhan, P.; Singh, N. Capacity optimization of grid connected solar/fuel cell energy system using hybrid ABC-PSO algorithm. *Int. J. Hydrog. Energy* **2020**, *45*, 10070–10088. [CrossRef]
26. Jamshidi, M.; Askarzadeh, A. Techno-economic analysis and size optimization of an off-grid hybrid photovoltaic, fuel cell and diesel generator system. *Sustain. Cities Soc.* **2018**, *44*, 310–320. [CrossRef]
27. Anoune, K.; Ghazi, M.; Bouya, M.; Laknizi, A.; Ghazouani, M.; Ben Abdellah, A.; Astito, A. Optimization and techno-economic analysis of photovoltaic-wind-battery based hybrid system. *J. Energy Storage* **2020**, *32*, 101878. [CrossRef]
28. Khan, A.; Javaid, N. Optimal sizing of a stand-alone photovoltaic, wind turbine and fuel cell systems. *Comput. Electr. Eng.* **2020**, *85*, 106682. [CrossRef]
29. El-Sattar, H.A.; Kamel, S.; Sultan, H.M.; Zawbaa, H.M.; Jurado, F. Optimal design of Photovoltaic, Biomass, Fuel Cell, Hydrogen Tank units and Electrolyzer hybrid system for a remote area in Egypt. *Energy Rep.* **2022**, *8*, 9506–9527. [CrossRef]
30. Zhao, W.; Wang, L.; Zhang, Z. Artificial ecosystem-based optimization: A novel nature-inspired meta-heuristic algorithm. *Neural Comput. Appl.* **2019**, *32*, 9383–9425. [CrossRef]
31. Long, W.; Jiao, J.; Xu, M.; Tang, M.; Wu, T.; Cai, S. Lens-imaging learning Harris hawks optimizer for global optimization and its application to feature selection. *Expert Syst. Appl.* **2022**, *202*, 117255. [CrossRef]
32. Askarzadeh, A. Electrical power generation by an optimised autonomous PV/wind/tidal/battery system. *IET Renew. Power Gener.* **2016**, *11*, 152–164. [CrossRef]
33. Hosseinalizadeh, R.; Shakouri, G.H.; Amalnick, M.S.; Taghipour, P. Economic sizing of a hybrid (PV-WT-FC) renewable energy system (HRES) for stand-alone usages by an optimization-simulation model: Case study of Iran. *Renew. Sustain. Energy Rev.* **2016**, *54*, 139–150. [CrossRef]
34. Available online: <https://solargis.com/maps-and-gis-data/download/malaysia> (accessed on 8 January 2023).
35. Hossain, M.Z.; Illias, H.A. Binary power generation system by utilizing solar energy in Malaysia. *Ain Shams Eng. J.* **2022**, *13*, 101650. [CrossRef]
36. Ramli, M.A.; Bouchekara, H.; Alghamdi, A.S. Optimal sizing of PV/wind/diesel hybrid microgrid system using multi-objective self-adaptive differential evolution algorithm. *Renew. Energy* **2018**, *121*, 400–411. [CrossRef]
37. Naderipour, A.; Abdul-Malek, Z.; Nowdeh, S.A.; Kamyab, H.; Ramtin, A.R.; Shahrokh, S.; Klemeš, J.J. Comparative evaluation of hybrid photovoltaic, wind, tidal and fuel cell clean system design for different regions with remote application considering cost. *J. Clean. Prod.* **2021**, *283*, 124207. [CrossRef]

Disclaimer/Publisher’s Note: The statements, opinions and data contained in all publications are solely those of the individual author(s) and contributor(s) and not of MDPI and/or the editor(s). MDPI and/or the editor(s) disclaim responsibility for any injury to people or property resulting from any ideas, methods, instructions or products referred to in the content.